Results in Engineering 24 (2024) 103032

Contents lists available at ScienceDirect

Results in Engineering

journal homepage: www.sciencedirect.com/journal/results-in-engineering

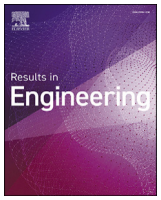

Research paper

Sliding mode control design using a generalized reduced-order fractional model for chemical processes

Juan J. Gude [a,*], Antonio Di Teodoro [b], D'hamar Agudelo [b], Marco Herrera [b], Luis Rincón [b], Oscar Camacho [b]

[a] Department of Computing, Electronics and Communication Technologies, Faculty of Engineering, University of Deusto, Bilbao, 48007, Bizkaia, Spain
[b] Colegio de Ciencias e Ingenierías "El Politécnico", Universidad San Francisco de Quito USFQ, Quito, 17057, Ecuador

ARTICLE INFO

Keywords:
Sliding mode control
Fractional-order model
Generalization procedure

ABSTRACT

This article presents a comprehensive study that evaluates the potential advantages of adopting a unified, systematic, and organized general fractional model within the Sliding Mode Control (SMC) design framework. The exploration extends to the model's applicability in a variety of disciplines. Although prior research has utilized SMC and fractional-order systems independently, no previous work has established a mathematical framework that integrates a generic fractional-order SMC model. The study addresses this gap and highlights potential implications for control design and applications in a variety of fields, particularly for chemical processes.

1. Introduction

Fractional-order systems and control structures have received increasing interest in the academic and industrial community in recent years, and there are many potential breakthroughs in this field [1,2]. Fractional-order systems use fractional calculus, which is the extension of traditional calculus that considers the derivation and integration of any order, not only integers. Academics and industry professionals widely acknowledge that these systems offer various advantages over traditional systems of integer order, including superior precision, robustness, and higher-order dynamics [3].

In the last four decades, fractional-order calculus has been used successfully in the modeling of physical phenomena and systems studied in many fields of science and engineering [4]. Among these, industrial chemical processes are particularly relevant [5–7], which have evolved to affect a variety of sectors, such as biomedicine, chemical engineering, environmental systems, materials engineering and technology.

In this context, fractional-order control structures use fractional-order models and controls to improve control systems' performance [8]. In a conventional control system, the controller uses an integer-order derivative to calculate the rate of change of the control signal. In contrast, in a fractional-order control system, the controller makes use of a fractional-order derivative. Fractional-order controllers offer several advantages compared to their integer-order counterparts [3]. For example, they can provide superior control performance, particularly in nonlinear or time-varying dynamic systems. In addition, they can improve system stability, reduce both overshoot and undershoot, and provide better tracking of desired setpoint values. Furthermore, fractional-order controllers can be tuned more easily than integer-order controllers, and they can be designed to achieve specific performance objectives [9].

In chemical engineering applications, fractional-order controllers can significantly improve control performance, demonstrating the potential of fractional systems and control structures in this engineering area. Some studies focus on developing analytical and design procedures to incorporate fractional-order integrodifferential operators into classical control systems [10,11]. This involves extending classical control theory to account for fractional-order dynamics and developing new analytical and design tools to deal with the resulting complexities [12,13]. Since the proportional-integral-derivative (PID) controller is currently the most dominant control algorithm in industry [14], a natural approach is to use a fractional-order PID controller, which extends the traditional integer-order PID controller by including fractional integral and derivative terms [15–17].

To design fractional-order control systems, a model of the controlled process is usually required. Developing a phenomenological model for many industrial processes is often difficult due to their complexity and the significant limitation of insufficient data on the process parameters. Most process models that link controlled and manipulated variables are of higher order, needing more complicated controllers mainly for ana-

* Corresponding author.
E-mail address: jgude@deusto.es (J.J. Gude).

https://doi.org/10.1016/j.rineng.2024.103032
Received 25 June 2024; Received in revised form 25 September 2024; Accepted 28 September 2024
Available online 2 October 2024

lytical purposes and the number of tuning parameters. Hence, a reduced-order model might be sufficient for design purposes [18].

Standard first-order plus dead-time (FOPDT) models can be considered a valuable resource in process control, as they facilitate system examination using straightforward low-order linear models with dead time. Their primary strength lies in their simplicity and ability to grasp the fundamental dynamics of various industrial processes. However, a limitation of these simplified models is the uncertainties they introduce, which can reduce the performance of traditional controllers [19].

Another approach involves employing fractional-order calculus to model and analyze complex systems. It is important to note that fractional-order differential equations are an excellent technique for describing many complex physical systems [3,20]. Fractional-order models can capture nonlinear and nonlocal dynamics that are difficult to depict using traditional integer-order models [21].

More specifically, the industry requires accurate methods to identify fractional models that are characterized by their simplicity of implementation and application [22]. In this particular context, the literature presents a broad range of techniques of identification for reduced-order fractional models. Some identification methods for fractional first-order plus dead-time (FFOPDT) models that have recently been proposed are listed below. Analytical techniques based on process response to a step-input signal, as proposed in [23] and [24], provide an effective proposal while remaining simple and easy to implement. The procedure outlined in [25] takes advantage of the asymptotic behavior of the Mittag-Leffler (ML) function to estimate more accurately the fractional order. Another common approach involves identification methods based on optimization algorithms [20,26,27]. The hybrid approach detailed in [28] combines analytical techniques with those based on optimization, revealing a balance between procedural simplicity and model accuracy. These types of identification procedures will facilitate the widespread implementation of reduced-order fractional models within industrial contexts [29]. More recently, a generalized approach based on the process reaction curve has been introduced to identify fractional second-order systems [30].

On the basis of the limitations of conventional controllers, an increasing number of researchers have integrated fractional theory into control systems in recent years. The goal is to increase the performance of the control system including fractional integral and derivative terms. Progress in applied fractional calculus and emerging computational techniques have led to the development of new control strategies considering fractional-order models. Consequently, the design of control systems based on fractional-order calculus requires developing novel tools and techniques [31]. For example, fractional-order optimization methods have been developed to tune fractional-order controllers [32], and fractional observers have been used to estimate the states of fractional systems [33]. In addition, simulation tools have been developed to simulate fractional-order systems and their corresponding control structures [34].

Control theory recognizes the structure of sliding mode control (SMC) as one of its widely studied topics [35]. SMC is a robust nonlinear control technique to synthesize controllers for linear and nonlinear processes [18,36]. The fundamental principle of SMC is to drive the system to a sliding surface, thus constraining the system dynamics to a specific subspace. The control input is configured to keep the system on the sliding surface, even in the presence of disturbances and uncertainty. This approach ensures the stability and robust performance of the system. Additionally, it also gives the SMC significant characteristics, serving as a robust control tool offering effective response to nonlinear systems with uncertainty. Thus, SMC is beneficial due to its insensitivity to deviations and perturbations of modeling that affect these systems [37–39]. SMC has been implemented in a variety of contexts, including chemical, electrical, mechanical, and aerospace systems, and has proven valuable in practical areas such as power systems, robotics, and vehicle control.

As mentioned above, the SMC guides the controlled variable from its initial state to a desired final state by employing a sliding surface that reflects the intended behavior of the process variable. Consequently, the process behavior of the process will be sensitive to the surface parameters [40,41]. Within the control law, the sliding surface plays a crucial role, comprising two components: the continuous (sliding part) and the discontinuous part (reaching part) [35,42,43]. Despite its advantages, SMC can be challenging to implement due to the chattering phenomenon. Chattering is a high-frequency oscillation in the control input when the system is close to the sliding surface. This can result in excessive wear and tear on mechanical systems and can cause electrical noise in electrical systems. Various modifications have been proposed to mitigate chattering, including boundary layer methods, smoothing techniques, adaptive control methods, and some in fractional sliding mode control [44].

The present study is motivated by the recent advances and the gradual introduction of fractional calculus at industrial level, the importance of fractional reduced-order models to characterize industrial processes, and its application in the framework of SMC to improve control performance of this control structure in chemical applications.

This paper presents a comprehensive study aiming at identifying the potential benefits of adopting a complete, schematic, and organized general fractional model in the context of SMC control design, as well as its potential applications in other areas. SMC and fractional-order systems have been used in different ways in previous research, but no mathematical framework encompassing a general fractional-order model has been developed. To the best of our knowledge, this is the first time that a generalization of a fractional-order model has been utilized to synthesize an SMC law, and different specific realizations of the control law are used to validate its effectiveness.

To summarize, the key contributions of this research are as follows:

1. Introduce a comprehensive and structured general fractional model in the context of SMC control technique.
2. Explore the potential benefits of using this general fractional-order model.
3. Examine the implications of the general fractional model in control design and its applicability in various fields. Finally, it validates the proposed control law through testing with specific implementations in chemical process.

The structure of this paper is organized as follows. Section 2 provides background information on fractional calculus. In Section 3, the generalization of the fractional Sliding Mode control law is presented, considering a general fractional reduced-order model. Section 4 considers some particular cases of the control law discussed in the previous section. An analysis of the stability is discussed in Section 5. Section 6 shows the numerical results when the designed control law is implemented in two application examples, a nonlinear mixing tank and a high-order linear system with a long time delay. Finally, conclusions are presented in Section 7.

2. Elements of the fractional calculus

2.1. Brief introduction to fractional calculus

Consider a finite interval $[a,b]$ on the real axis $\mathbb{R}$. The Riemann–Liouville fractional integral of order $\alpha > 0$ is expressed as (refer to [45–48]):

$$\left(I_{a^+}^{\alpha} h\right)(x) = \frac{1}{\Gamma(\alpha)} \int_a^x \frac{h(t)}{(x-t)^{1-\alpha}}\, dt, \quad x > a, \tag{1}$$

where $\Gamma(\alpha)$ is the Gamma function. Let $I_{a^+}^{\alpha}(L_1)$ denote the collection of functions h represented by (1) of a summable function, where $h = I_{a^+}^{\alpha}\varphi$ and $\varphi \in L_1(a,b)$. Note that a comprehensive description of these functions can be found in [45,48]. We denote the classical integral as I.

Theorem 1. *A function $h \in I^{\alpha}_{a^+}(L_1(a,b)), \alpha > 0$, if and only if $I^{l-\alpha}_{a^+} h \in AC^l([a,b])$, $l = [\alpha]+1$ and $(I^{l-\alpha}_{a^+} h)^{(k)}(a) = 0$, $k = 0, \dots, l-1$.*

$AC^l([a,b])$ represents the set of functions h that are continuously differentiable within the interval $[a,b]$, up to order $l-1$, and $h^{(l-1)}$ is absolutely continuous in $[a,b]$. Removing the final condition from Theorem 1 yields a set of functions permitting a summable fractional-order derivative.

Definition 1 *(Refer to [48]).* For a function $h \in L_1(a,b)$ to have a summable fractional-order derivative $\left(D^{\alpha}_{a^+} h\right)(x)$, it must satisfy the condition:

$$\left(I^{l-\alpha}_{a^+} h\right)(x) \in AC^l([a,b]),$$

where $l = [\alpha]+1$.

Definition 2. For $\alpha \geq 0$ and $l = [\alpha]+1$, the operator $\mathcal{D}^{\alpha}_{a^+}$ is defined as follows: $\left(\mathcal{D}^{\alpha}_{a^+} f\right)(t) := \left(\frac{d}{dx}\right)^l (I^{l-\alpha}_{a^+} f)(t)$, whenever $f \in L_1[a,b]$.

Some important results that facilitate in advancing fractional theory concern the composition of operators, a concept not universally valid; hence, it is necessary to carefully consider the hypotheses required for the function.

Lemma 1. *If $\Re(\alpha) > 0$ and $f(x) \in L_p(a,b)$, with $(1 \leq p \leq \infty)$, then the following equalities*

$$(D^{\alpha}_{a^+} I^{\alpha}_{a^+} f)(x) = f(x) \quad \text{and} \quad (D^{\alpha}_{a^-} I^{\alpha}_{a^-} f)(x) = f(x) \quad (\Re(\alpha) > 0), \tag{2}$$

hold almost everywhere on $[a,b]$. (See the proof in [48].)

Lemma 2. *Let $\Re(\alpha) > 0$, $n = [\Re(\alpha)]+1$ and let $f_{n-\alpha} = (I^{n-\alpha}_{a^+} f)(x)$ be the Riemann-Liouville fractional integral of order $n-\alpha$.*

If $1 \leq p \leq \infty$ and $f(x) \in I^{\alpha}_{a^+}(L_p)$, then

$$(I^{\alpha}_{a^+} D^{\alpha}_{a^+} f)(x) = f(x). \tag{3}$$

(See the proof in [48].)

2.2. Laplace transform of fractional-order derivatives

Definition 3. Consider $F(s) := (\mathscr{L} f)(s)$ to represent the Laplace transform of certain function f, $\boldsymbol{\alpha} \in (n-1, n]$, and $n \in \mathbb{N}$ (see [48]).

$$\left(\mathcal{L}\ D^{\alpha}_{0^+} f\right)(s) = s^{\alpha} F(s) - \sum_{k=1}^{n} s^{k-1} (D^{\alpha-k}_{0^+} f)(0)$$

Note that the semigroup property for the composition of fractional derivatives is not universally applicable (refer to [47, Sect. 2.3.6]). Specifically, the property:

$$D^{\eta}_{a^+}\left(D^{\gamma}_{a^+} h\right) = D^{\eta+\gamma}_{a^+} h, \tag{4}$$

holds under the conditions:

$$h^{(j)}(a^+) = 0, \qquad j = 0, 1, \dots, s-1, \tag{5}$$

where $h \in AC^{s-1}([a,b])$, $h^{(s)} \in L_1(a,b)$ and $s = [\gamma]+1$. This result can be summarized in the following lemma:

Lemma 3. *Let $h \in AC^{s-1}([a,b])$ and $h^{(s)} \in L_1(a,b)$. Then, the equation*

$$D^{\eta}_{a+}\left(D^{\gamma}_{a+}\right) h = D^{\gamma}_{a+}\left(D^{\eta}_{a+}\right) h, \tag{6}$$

holds provided that

$$h^{(j)}(a^+) = 0, \quad j = 0, 1, \dots, s-1, \tag{7}$$

where $s = [\gamma]+1$.

Proof. Refer to [47, Sect. 2.3.6] for the proof. □

3. Theoretical mathematical model

This section presents a generalization of the fractional-order sliding mode control law, considering a general fractional reduced-order model. The reaction curve is achieved using an open-loop procedure [49], which involves subjecting the process to a step-type change, approximately 10% around the operating value in the controller output. The model parameters are determined using the methods presented by Gude et al. [25,22].

It is important to note that this model is obtained solely for the design of control laws and will not be subject to subsequent abrupt changes. In addition, most chemical processes are in the regulation mode, which means that the rejection of disturbances is the main control activity. The natural robustness of the SMC compensates for the uncertainties in the model.

Remark 1. Although the model provides a generalized representation of the process, this paper prioritizes simpler cases for both examples and numerical implementation. Utilizing a broad framework for straightforward problems might appear contradictory, however, our aim is to thoroughly comprehend the model, scrutinize the theorems, and assure precise mathematical computations. Given that the model represents overdamped systems, it has potential uses in chemical processes and mobile robotics.

This section is organized as follows. In Section 3.1, the mathematical objects necessary to better understand the generalization of the reduced-order fractional model are defined. Section 3.2 presents a generalization of the fractional-order SMC control law considering a general model, which is expressed in the form of a rational transfer function with multiple fractional parameters.

3.1. Introduction of the mathematical objects

Before defining our model, let us define the following mathematical objects that will help us better understand generalization.

Considering

$$\sum_{\alpha_1 < \cdots < \alpha_m} a_{\alpha_1} X^{\alpha_1} \cdots a_{\alpha_m} X^{\alpha_m},$$

where the variable X^{α_j} corresponds to the fractional derivative or integral of order α_j in terms of the vectorial representation $(X^{\alpha_1}, \dots, X^{\alpha_n})$. We introduce the abbreviations

$$X^{\alpha_1} X^{\alpha_2} = X^{\alpha_1+\alpha_2},\ X^{\alpha_2} X^{\alpha_3} = X^{\alpha_2+\alpha_3},\ \dots,\ X^{\alpha_1} \cdots X^{\alpha_n} = X^{\alpha_1+\cdots+\alpha_n}$$

A is a set of all combinations of m indices $\alpha_1, \dots, \alpha_m$ with $1 \leq \mu_1 < \cdots < \mu_m \leq n$.

Example 1. Consider the considered set $A = \{\alpha_1, \alpha_2, \alpha_3, \alpha_1+\alpha_2, \alpha_1+\alpha_3, \alpha_2+\alpha_3, \alpha_1+\alpha_2+\alpha_3\}$. Then $S_{\alpha}(\cdot) = a_0 + a_1 D^{\alpha_1} + a_2 D^{\alpha_2} + a_3 D^{\alpha_3} + a_{12} D^{\alpha_1+\alpha_2} + a_{23} D^{\alpha_2+\alpha_3} + a_{13} D^{\alpha_1+\alpha_3} + a_{123} D^{\alpha_1+\alpha_2+\alpha_3}$. Parameter α_0 is the identity element of A.

The parameters $\alpha_A \in A$ represent all possible combinations of sums, as shown in the example. With this in mind, we can define the operator that we will use throughout this paper. The Riemann-Liouville operator $D^{\alpha_A}_{a^+}$

$$\left(\mathfrak{D}^{\alpha_A}_{a^+} f\right)(t) := \left(D^{\alpha_A}_{a^+} f\right)(t) = \left(\frac{d}{dx}\right)^l (I^{l-\alpha_A}_{a^+} f)(t) \tag{8}$$

This operator satisfies the following conditions:

- $D^{\alpha_0}(\cdot) = (\cdot)$
- $I^{n-\alpha_0}(\cdot) = (\cdot)$
- If $\max\{\alpha_A\} \leq 1$ means that $\sum_i^n \alpha_i \leq 1$. Then

$$\left(D_{a^+}^{\alpha_A} f\right)(t) = \left(\frac{d}{dx}\right)\left(I_{a^+}^{1-\alpha_A} f\right)(t), \tag{9}$$

$n \in \mathbb{N}$ is connected with the transfer function.

On the other hand, consider the operator σ decomposed into a differential part S_α and an integral part I_α expressed in terms of the fractional-order derivative operator as follows:

$$\sigma[X, Y] := \Phi S_\alpha[X, Y] + \Psi I_\alpha[X, Y] \tag{10}$$

where $S_\alpha, I_\alpha \in AC^1(\mathbb{R}\times\mathbb{R}, \mathbb{R})$, Φ and Ψ are real constants, and σ can be considered as a real-valued function $\sigma : \mathbb{R}\times\mathbb{R} \to \mathbb{R}$. Our operators S_α and I_α can be written in the following form:

$$S_\alpha(\cdot) = \sum_A a_A \mathfrak{D}^{\alpha_A}(\cdot), \tag{11}$$

$$I_\alpha(\cdot) = \sum_A b_A \mathfrak{I}^{n-\alpha_A}(\cdot) \tag{12}$$

where $n = [\alpha_A]+1$ and a_A and b_A are real numbers. $\mathfrak{D}^{\alpha_A}$ is the fractional derivative in some sense and $\mathfrak{I}^{n-\alpha_A}$ is the Riemann-Liouville integral.

3.2. Rational model functions $\frac{p}{q}$ with $p \in \mathbb{R}$ and multiple fractional parameters

In this section, a generalization of the fractional-order SMC control law is proposed by considering a general model in the form of a rational transfer function with multiple fractional parameters. To proceed with this development, we will first define the sliding surface function. Taking into account equation (10) and the function e, secondly, we will propose a general form for G. This function generalizes any rational model of the form constant over exponential. Thirdly, we will adapt σ to the form of G under certain conditions, for which we will propose and demonstrate a key proposition. Fourthly, we will conclude with a theorem that completes the cycle and allows, under certain assumptions, the use of this method by simply applying the theorem as seen in the example later on.

Definition 4. Consider $e, Ie \in AC^1(\mathbb{R}, \mathbb{R})$ functions. Using (10), the sliding surface function $\sigma_\alpha[e, Ie]$ is defined as:

$$\sigma_\alpha[e, Ie](t) = \Phi S_\alpha[e, Ie](t) + \Psi I_\alpha[e, Ie](t). \tag{13}$$

We introduce the operator $\mathbf{T}$ as follows:

$$\mathbf{T}(X) := (X, Y) = X + IY, \tag{14}$$

in consequence:

$$\mathbf{T}(e) := (e, Ie) = c_d e + c_i Ie, \tag{15}$$

where $c_d, c_i \in \mathbb{R}$ and $I(\cdot)$ represents the classical Riemann integral.

Consider the following function $G(s) : \mathbb{R} \to \mathbb{R}$, defined as:

$$G(s) := \frac{K}{\prod_{i=1}^{n} \exp(p_i s^{\alpha_i})} = \frac{K}{\prod_{i=1}^{n}\sum_{k=0}^{\infty} \frac{(p_i s^{\alpha_i})^k}{k!}}, \tag{16}$$

where $p_i \in \mathbb{R}$ and $\alpha_i \in [a, b]$ (fractional parameter) for each $i \in \mathbb{N}$.

Example 2. The case considering $n = 2$, $p_1 = T$, $p_2 = L$, $\alpha_1 = \alpha$, and $\alpha_2 = 1$ is the most studied case and corresponds to the transfer function of the FFOPDT model [22]:

$$G(s) = \frac{K}{\exp(Ts^\alpha)\exp(Ls)}. \tag{17}$$

We now provide a first-order approximation for the function $G(s)$ from eq. (16):

$$G(s) = \frac{K}{\prod_{i=1}^{n}\left(\frac{(p_i s^{\alpha_i})^0}{0!} + \frac{(p_i s^{\alpha_i})^1}{1!} + r_i\right)}, \tag{18}$$

where r_i is the i-th component associated with the truncation of order i in the Taylor series expansion. Thus, the expression can be simplified:

$$G(s) = \frac{K}{\prod_{i=1}^{n}\left(1 + p_i s^{\alpha_i} + r_i\right)}. \tag{19}$$

Remark 2. The expression (19) represents a generalization form of a function $\frac{p}{q}$ such that $p \in \mathbb{R}$ and $q = Q(s)$. Note that the differentiability problems occur only at the zeros of Q.

Proposition 1. *Consider $G(s) = \frac{X(s)}{U(s)}$ and the hypothesis of Lemma 3*

$$G(s) = \frac{K}{\prod_{i=1}^{n}\sum_{k=0}^{\infty} \frac{(p_i s^{\alpha_i})^k}{k!}}.$$

Then, we have:

$$X(t) + \prod_{i=1}^{n}\sum_{k=1}^{\infty} \frac{p_i^k}{k!} D^{k\alpha_i} X(t) = U(t)K, \tag{20}$$

where $D^{k\alpha_i}$ represents the fractional derivative of order $k\alpha_i$ (note that $D^{0\alpha_i}(\cdot) = D^0(\cdot) = (\cdot)$).

Proof. Let $G(s)$ define as:

$$G(s) = \frac{X(s)}{U(s)} = \frac{K}{\prod_{i=1}^{n}\sum_{k=0}^{\infty} \frac{(p_i s^{\alpha_i})^k}{k!}}. \tag{21}$$

This implies:

$$X(s)\prod_{i=1}^{n}\sum_{k=0}^{\infty} \frac{(p_i s^{\alpha_i})^k}{k!} = U(s)K. \tag{22}$$

The above proposition establishes the relationship existing between the transfer function $G(s)$ and the expressions for $X(s)$ and $U(s)$.

Due to the convergence property of power series and Lemma 3, we can write the following relation:

$$D^{\alpha_i}\sum_{k=0}^{\infty}(p_i s^{\alpha_i})^k = \sum_{k=0}^{\infty} D^{\alpha_i}(p_i s^{\alpha_i})^k = \sum_{k=0}^{\infty} D^{\alpha_i}(p_i^k s^{k\alpha_i}). \tag{23}$$

Applying the Laplace inverse transform $\mathcal{L}^{-1}$ to eq. (22), while assuming that $\sum_{k=1}^{n} s^{k-1}(D_{0^+}^{\alpha_i - k} X)(0) = \epsilon$ such that $\epsilon \to 0$ for each $n \in \mathbb{N}$, results in the following expression:

$$\prod_{i=1}^{n}\sum_{k=0}^{\infty} \frac{p_i^k}{k!} D^{k\alpha_i} X(t) = U(t)K. \tag{24}$$

Remark 3. Note that these conditions ($\sum_{k=1}^{n} s^{k-1}(D_{0^+}^{\alpha_i - k} X)(0) = \epsilon$) are required in the case where the fractional parameters reside in an interval (a, b). However, in the case where they are in $(0, 1)$, it is sufficient to request the initial condition only on the function ($X(0) = \epsilon$).

We are aware of the difficulty posed by initial conditions in fractional calculus, due to its non-locality. However, this is a much more

advanced topic of discussion that falls outside the scope of this paper, as we impose the condition $max(\sum_A \alpha_A) \leq 1$, seeking to make the implementation much simpler.

On the other hand, and merely aiming to generate future discussions on the treatment of initial conditions in fractional calculus, one could consider sets of functions (polynomials, for example) that ensure the solution of initial value problems. □

Consider the error signal $e(t)$, which is defined as follows:

$$e(t) = R(t) - X(t), \tag{25}$$

where $R(t)$ is the setpoint, specifying desired operating values for tracking changing references or rejecting disturbances, and $X(t)$ is the process output or controlled variable, representing actual output values. Error information is fundamental in SMC as it uses feedback to adjust the process and ensure it meets the desired specifications, whether tracking changing references or regulating against disturbances. Both functions $R(t)$ and $X(t)$ belong to $AC^n([a,b]), n \in \mathbb{N}$.

In consequence,

$$\frac{d}{dt}e = \dot{e} = \dot{R} - \dot{X}, \tag{26}$$

$$Ie = IR - IX. \tag{27}$$

Now, we analyze the implications of $\mathbf{T}(e)$.

$$\mathbf{T}(e) = \mathbf{T}R - \mathbf{T}X. \tag{28}$$

$$\mathbf{T}(e) = (R - X, IR - IX) = R - X + IR - IX =$$
$$R + IR - (X + IX) = \mathbf{T}R - \mathbf{T}X.$$

The following proposition is needed to continue our development; its proof is quite straightforward.

Proposition 2. *Consider $\alpha_A \geq 0$, $\alpha_A \in A$ and $n_A = [\alpha_A] + 1$. The derivative of $\sigma_\alpha[X, Y]$ with respect to time t is zero if and only if:*

$$\left(\Phi \sum_A a_A \left(\frac{d}{dt}\right)^{n_A+1} + \Psi \sum_A b_A \frac{d}{dt}\right) I^{n_A-\alpha_A}(\boldsymbol{T}(e)) = 0. \tag{29}$$

On the other hand, if $\mathcal{D}_t^{n_A} = \Phi \sum_A a_A \left(\frac{d}{dt}\right)^{n_A+1} + \Psi \sum_A b_A \frac{d}{dt}$. Then, we can rewrite (29) as:

$$\mathcal{D}_t^{n_A} I^{n_A-\alpha_A}(\boldsymbol{T}(e)) = 0. \tag{30}$$

Proof. Using linearity:

$$\frac{d}{dt}\sigma_\alpha(\mathbf{T}(e)) = \tag{31}$$
$$\frac{d}{dt}\sigma_\alpha[e, Ie] =$$
$$\Phi \frac{d}{dt} S_\alpha[e, Ie] + \Psi \frac{d}{dt} I_\alpha[e, Ie] =$$
$$\Phi \sum_A a_A \frac{d}{dt} D^{\alpha_A}(e, Ie) + \Psi \sum_A b_A \frac{d}{dt} I^{n-\alpha_A}(e, Ie) = 0.$$

Finally, using the definition of the fractional derivative, we get the result. □

The following particular cases serve to apply to specific models (whether known or unknown. For example, of order $\alpha_1 + \alpha_2$) and to understand how the proposition works.

Particular Cases:

1. When $n_A = 1$, (29) reduces to:

$$\left(\Phi \sum_A a_A \left(\frac{d}{dt}\right)^2 + \Psi \sum_A b_A \frac{d}{dt}\right) I^{1-\alpha_A}(e, Ie) = 0. \tag{32}$$

2. Using I in the equation (29) instead of $I^{n_A-\alpha_A}$:

$$\Phi \sum_A a_A \left(\frac{d}{dt}\right)^n [e, Ie] + \Psi \sum_A b_A [e, Ie] = 0. \tag{33}$$

3. Using I in the equation (29) instead of $I^{n_A-\alpha_A}$ and $n_A = 2$:

$$\Phi \sum_A a_A \left(\frac{d}{dt}\right)^2 [e, Ie] + \Psi \sum_A b_A [e, Ie] = 0. \tag{34}$$

Remark 4. Two conditions to discuss: the first is that $max(\sum_A \alpha_A) \leq 1$ serves to simplify the model when calculating and computationally implementing it; however, in this paper, the model is developed in a general way. The second is that taking $n_A = \lceil \alpha_A \rceil + 1$ ensures that each of the indices of $\alpha_A \in A$ meets the condition. For example, if we work with two fractional indices α_1, α_2, the condition requires that $n_1 = \alpha_1 + 1$, $n_2 = \alpha_2 + 1$, but also $n_{12} = (\alpha_1 + \alpha_2) + 1$. Consider that $n = n_A = [\alpha_A] + 1$.

By using Proposition 2 and the operator $\mathbf{T}$ applied to e, we have the following relationship:

$$\Phi \sum_A a_A \frac{d}{dt} D^{\alpha_A}(\mathbf{T}R - \mathbf{T}X) + \Psi \sum_A b_A \frac{d}{dt} I^{n-\alpha_A}(\mathbf{T}R - \mathbf{T}X) = 0.$$

In summary, under the general control law study and when the operator $\mathbf{T}$ is applied to the error e, it leads to the relationship $\dot{\sigma_\alpha}(T(e)) = 0$.

In consequence, we can write the following system:

$$\begin{cases} \prod_{i=1}^{n} \sum_{k=0}^{\infty} \frac{p_i^k}{k!} D^{k\alpha_i} X(t) = U(t)K, \\ \Phi \sum_A a_A \frac{d}{dt} D^{\alpha_A}(\mathbf{T}R - \mathbf{T}X) + \Psi \sum_A b_A \frac{d}{dt} I^{n-\alpha_A}(\mathbf{T}R - \mathbf{T}X) = 0 \end{cases} \tag{35}$$

or equivalently,

$$\begin{cases} \prod_{i=1}^{n} \sum_{k=0}^{\infty} \frac{p_i^k}{k!} D^{k\alpha_i} X(t) = U(t)K, \\ \mathcal{D}_t^{n_A} I^{n_A-\alpha_A}(\mathbf{T}R - \mathbf{T}X) = 0. \end{cases} \tag{36}$$

With all the results previously displayed, we can formulate the following theorem:

Theorem 2. *Let A be a set of all combinations of m indices $\alpha_1, \ldots, \alpha_m$, $X, R \in L_1(a,b)$, $\alpha_A \in (a,b)$ and $a_A, b_A, \Phi, \Psi \in \mathbb{R}$. Under the hypothesis of Lemma 3 and $D^0(\cdot) = D^{0\alpha_i}(\cdot) = c_i$, where $c_i \in \mathbb{R}$ for each $i \in \mathbb{N}$. Then, the control law in the Riemann-Liouville sense is provided by:*

$$U(t) =$$
$$\frac{1}{K}\left[\prod_{i=1}^{n} \sum_{k=0}^{\infty} \frac{p_i^k}{k!} D^{k\alpha_i} X(t) - \mathcal{D}_t^{n_A} I^{n_A-\alpha_A}(R + IR - (X + IX))\right].$$

Considering $\theta \leq n$ and the truncation error of the exponential function equal to zero, we get the following expression:

$$U(t) =$$
$$\frac{1}{K}\Big[\prod_{i=1}^{n} \sum_{k=0}^{\infty} \frac{p_i^k}{k!} D^{k\alpha_i} X(t) -$$
$$\left(\sum_{k\in A} \Phi a_k \frac{d}{dt} D^{\alpha_k} + \Psi b_k \frac{d}{dt} I^{n_k-\alpha_k}\right) \cdot \left(R + IR - (X + IX)\right)\Big]. \tag{37}$$

The explicit matrix form for (37), which is very useful for implementation purposes, is:

$$KU(t) = \left(\prod_{i=1}^{n}\sum_{k=0}^{\theta}\frac{p_i^k}{k!}D^{k\alpha_i} \quad -\Big(\sum_{k\in A}\Phi a_k\frac{d}{dt}D^{\alpha_k}+\Psi b_k\frac{d}{dt}I^{n_k-\alpha_k}\Big)\right)\cdot \begin{pmatrix} X \\ R+IR-(X+IX)\end{pmatrix} \tag{38}$$

Here, $\theta \le n$ is a parameter that governs the truncation of the exponential power series expansion. It is worth noting that, in practice, the value of θ is taken to be large, approaching infinity, to ensure accurate results. In addition, n denotes the number of exponential functions involved in the operators S_α and I_α.

4. Particular cases

In this section, we consider several particular cases of the control law given in Theorem 2.

The structure of this section is as follows: Section 4.1 deals with the classical approach to the fractional-order SMC control law, assuming the fractional parameters approach one. In Section 4.2, the control law is particularized for the case of transfer functions with two exponential functions, which is an interesting case due to its relevance to the FFOPDT model. Finally, Section 4.3 formulates the explicit general case involving n exponential functions.

4.1. Several cases and classical approach

The limit will be taken as the fractional parameters tend to one, with the idea of showing what the control law looks like in the classical case (that is, with integer parameters) to guide the reader on how the model looks in a particular case.

Case 1: Consider $n=\theta=1$, $A=\{\alpha_1\}$. Using the explicit matrix form of Theorem 2. Then we have:

$$KU(t) = \left(c_0+p_1D^{\alpha_1} \quad -\Big(\sum_{k=0}^{1}\Phi a_k\frac{d}{dt}D^{\alpha_k}+\Psi b_k\frac{d}{dt}I^{n_k-\alpha_k}\Big)\right)\cdot \begin{pmatrix} X \\ R+IR-(X+IX)\end{pmatrix}$$

where $c_i = c_0$.

Case 2: Consider $\Psi=0$, $n=2$, $\theta=1$ and $A=\{\alpha_1,\alpha_2,\alpha_1+\alpha_2\}$. Using the explicit matrix form of Theorem 2. Then we have:

$$KU(t) = \left(\prod_{i=1}^{2}\sum_{k=0}^{1}\frac{p_i^k}{k!}D^{k\alpha_i} \quad -\sum_{k\in A}\Phi a_k\frac{d}{dt}D^{\alpha_k}\right)\cdot\begin{pmatrix} X \\ R+IR-(X+IX)\end{pmatrix} = \left(\prod_{i=1}^{2}\Big(c_i+p_iD^{\alpha_i}\Big) \quad -\sum_{k\in A}\Phi a_k\frac{d}{dt}D^{\alpha_k}\right)\cdot\begin{pmatrix} X \\ R+IR-(X+IX)\end{pmatrix} = \Big(\Big(c_1+p_1D^{\alpha_1}\Big)\Big(c_2+p_2D^{\alpha_2}\Big) \quad -\Phi\Big(a_1\frac{d}{dt}D^{\alpha_1}+a_2\frac{d}{dt}D^{\alpha_2}+a_{12}\frac{d}{dt}D^{\alpha_1+\alpha_2}\Big)\Big)\cdot\begin{pmatrix} X \\ R+IR-(X+IX)\end{pmatrix} \tag{39}$$

Taking $\lim_{\alpha_i\to 1}U(t)$, for $i=1,2$, we get:

$$K\lim_{\alpha_i\to 1}U(t) = \lim_{\alpha_i\to 1}\Big(c_1c_2+c_1p_2D^{\alpha_2}+c_2p_1D^{\alpha_1}+p_1p_2D^{\alpha_1+\alpha_2}\Big)X- \Phi\lim_{\alpha_i\to 1}\Big(a_1\frac{d}{dt}D^{\alpha_1}+a_2\frac{d}{dt}D^{\alpha_2}+a_{12}\frac{d}{dt}D^{\alpha_1+\alpha_2}\Big)\Big(R+IR-(X+IX)\Big) = \Big(c_1c_2+(c_1p_2+c_2p_1)\frac{d}{dt}+p_1p_2\frac{d^2}{dt^2}\Big)X- \Big((a_1+a_2)\frac{d^2}{dt^2}+a_{12}\frac{d^3}{dt^3}\Big)\Big(R+IR-(X+IX)\Big) \tag{40}$$

Case 3: Consider $\Phi=0$, $n=2$, $\theta=1$ and $A=\{\alpha_1,\alpha_2,\alpha_1+\alpha_2\}$. Using the explicit matrix form of Theorem 2. Then we have:

$$KU(t) = \left(\prod_{i=1}^{2}\sum_{k=0}^{1}\frac{p_i^k}{k!}D^{k\alpha_i} \quad -\sum_{k\in A}\Psi b_k\frac{d}{dt}I^{n_k-\alpha_k}\right)\cdot\begin{pmatrix} X \\ R+IR-(X+IX)\end{pmatrix}$$

Case 4: Consider the function (39) of the case 2. And taking the following limits process $\alpha_1+\alpha_2\to 1, \alpha_1\to\frac{1}{2}, \alpha_2\to\frac{1}{2}$. Then we have:

$$KU(t) = \Big(\Big(c_1+p_1D^{\frac{1}{2}}\Big)\Big(c_2+p_2D^{\frac{1}{2}}\Big) \quad -\Phi\Big(a_1\frac{d}{dt}D^{\frac{1}{2}}+a_2\frac{d}{dt}D^{\frac{1}{2}}-+a_{12}\frac{d}{dt}D^{1}\Big)\Big)\cdot\begin{pmatrix} X \\ R+IR-(X+IX)\end{pmatrix}$$

4.2. Two exponential function case

This particular case is the most studied and approximates the transfer function of the FFOPDT model [22].

Consider the transfer function of the model (16) given by two exponentials ($n=2$):

$$G(s) = \frac{K}{\prod_{i=1}^{2}\sum_{k=0}^{\infty}\frac{(p_is^{\alpha_i})^k}{k!}}.$$

Truncating the series at $k=1$ and assuming that the truncation error is zero, we obtain the following rational transfer function:

$$G(s) = \frac{X(s)}{U(s)} = \frac{K}{\prod_{i=1}^{2}\left(1+p_is^{\alpha_i}\right)}. \tag{41}$$

Remark 5. Despite the unnecessary use of the product notation in this case to represent the product of only 2 binomials, we will employ it as it is simpler and helps to understand the subsequent generalization.

Notice that the denominator $Q(s)$ of $G(s)$ can be expressed as:

$$Q(s) = \prod_{i=1}^{2}\left(1+p_is^{\alpha_i}\right), \tag{42}$$

and we can observe the following properties:

1. $Q(s)=0$ if and only if $p_is^{\alpha_i}=-1$, which is equivalent to $s^{\alpha_i}=\frac{-1}{p_i}$ with $p_i\neq 0$ for each $i=1,\ldots,n$.
2. The degree of $Q(s)$ is given by $grad(Q(s))=\sum_{i=1}^{n}\alpha_i$ for the general case, and $grad(Q(s))=\alpha_1+\alpha_2$ for the specific case mentioned above.

By using Theorem 2, with $\theta=1<n=2$ and $\Psi=\Phi=1$, we obtain:

$$KU(t) = \left(\prod_{i=1}^{2}\sum_{k=0}^{1}\frac{p_i^k}{k!}D^{k\alpha_i} \quad -\Big(\sum_{k\in A}a_k\frac{d}{dt}D^{\alpha_k}+b_k\frac{d}{dt}I^{n_k-\alpha_k}\Big)\right)\cdot\begin{pmatrix} X \\ R+IR-(X+IX)\end{pmatrix}$$

4.3. Explicit general case

In this section, the fractional-order SMC control law is obtained by considering a general model in the form of a rational transfer function with multiple fractional parameters.

Consider the transfer function of the general model (16) given by n exponential functions:

$$G(s) = \frac{X(s)}{U(s)} = \frac{K}{\prod_{i=1}^{n}\left(1 + p_i s^{\alpha_i}\right)}, \tag{43}$$

where $K \in \mathbb{R}$. By using Theorem 2, with $\theta < n$ and $\Psi = \Phi = 1$. We derive the control law.

$$KU(t) = \left[\prod_{i=1}^{n}\sum_{k=0}^{1}\frac{p_i^k}{k!}D^{k\alpha_i}X(t) - D_t^{n_A}I^{n_A-\alpha_A}(R + IR - (X + IX))\right] = \left[\prod_{i=1}^{n}\left(c_i + p_i D^{\alpha_i}\right)X(t) - \sum_{k\in A}\frac{d}{dt}\left(a_k D^{\alpha_k} + b_k I^{1-\alpha_k}\right)\right]$$

Note that the series is truncated in our last model at order 1, yet we have n fractional indices whose sum can be equal 1. The intriguing aspect of the proposal is its flexibility, although numerical implementation might be challenging or even impossible.

5. Stability (convergence condition)

This section explores the concept of stability, extending it beyond the classical framework, and focusing specifically on Lyapunov stability. Understanding the role of stability in a broader context can be challenging and abstract. Therefore, it becomes crucial to scrutinize the explicit form of objects to ensure stability. However, we will elucidate a path that navigates through the classical approach while incorporating more general objects.

In the context of SMC systems, stability is obtained when two conditions are met: a) the stability of the sliding surface, which depends on the choice of parameters a_A, and b) reaching the sliding surface within a finite time, guaranteed by satisfying the reachability criterion.

Consider the discontinuous or switching part of the controller $U_d(t)$, which can be defined as:

$$U_d(t) = K_D sgn(\sigma(t)). \tag{44}$$

The complete control law is provided by:

$$U(t) = \frac{1}{K}\left[\prod_{i=1}^{n}\sum_{k=0}^{\infty}\frac{p_i^k}{k!}D^{k\alpha_i}X(t) - \Phi\sum_{A}a_A\frac{d}{dt}D^{\alpha_A}(R + IR - (X + IX)) - \Psi\sum_{A}b_A\frac{d}{dt}I^{n-\alpha_A}(R + IR - (X + IX))\right] + U_d(t).$$

Considering

$$\sigma_\alpha[e, Ie](t) := \Phi S_\alpha[e, Ie](t) + \Psi I_\alpha[e, Ie](t), \tag{45}$$

and equations (11) and (12),

$$\sigma_\alpha[e, Ie](t) = \Phi\sum_{A}a_A D^{\alpha_A}(e, Ie) + \Psi\sum_{A}b_A I^{n-\alpha_A}(e, Ie). \tag{46}$$

Using

$$e = R - X, \tag{47}$$

we can rewrite (46) as:

$$\sigma_\alpha[e, Ie](t) = \Phi\sum_{A}a_A D^{\alpha_A}(R + IR - (X + IX)) + \Psi\sum_{A}b_A I^{n-\alpha_A}(R + IR - (X + IX)). \tag{48}$$

At this point, one can observe the need for an explicit model to properly study stability. Calculating $\frac{d}{dt}\sigma_\alpha[e, Ie](t)$ in relation to the considered model, the following expression is obtained:

$$\frac{d}{dt}\sigma_\alpha[e, Ie](t) = \Phi\frac{d}{dt}S_\alpha[e, Ie](t) + \Psi\frac{d}{dt}I_\alpha[e, Ie](t) = \Phi\frac{d}{dt}\sum_{A}a_A D^{\alpha_A}(R + IR - (X + IX)) + \Psi\frac{d}{dt}\sum_{A}b_A I^{n-\alpha_A}(R + IR - (X + IX)). \tag{49}$$

Using Proposition 1, through algebraic manipulations and an explicit model, it could be seen that the equation

$$\frac{d}{dt}\sigma_\alpha[e, Ie](t)\sigma_\alpha[e, Ie](t) < 0$$

holds.

Remark 6. The handling of a model with abrupt changes must be approached from a distributional perspective. Although the theoretical mathematical model requires functions with favorable properties in terms of differentiability or integrability, from a practical and experimental standpoint, the step or impulse (a distributional derivative of the step) is omitted due to its practically negligible contribution to performance, given its very short duration and the detrimental effect to the final control element. In other words, from an experimental implementation perspective, responses with steps or impulses are treated as a continuous model; therefore, our model is applicable.

6. Application examples

To investigate the feasibility of the designed control law, numerical simulations are implemented by applying it in a nonlinear model and analyzing the performance when the process works in regulation mode. Additionally, the proposed controller is applied to a high-order linear system with a long time delay. The results were acquired through simulation with Matlab-Simulink.

Remark 7. As expected, two particular cases were used for computational implementation. The purpose was to demonstrate the flexibility of the theoretical proposal, but crucially to evaluate it against existing results, and thus confirm its efficacy.

6.1. Mixing tank process

A nonlinear mixing tank process [18] is considered, as illustrated in Fig. 1. The tank is fed by two streams: a hot flow $W_1(t)$ at a temperature $T_1(t)$, and a cold flow $W_2(t)$ at a temperature $T_2(t)$. A temperature transmitter positioned 125 [ft] from the tank determines the temperature of the outflow ($T_4(t)$).

The control system is designed to keep the mixing temperature $T_3(t)$ stable despite fluctuations in hot flow $W_1(t)$. This is achieved by manipulating the fail-close valve (FC) to adjust the cold flow $W_2(t)$. Furthermore, the temperature transmitter is calibrated to measure within a range of 100 to 200 [F]. For the interested reader, the complete description of the nonlinear model, the steady-state parameters, and the system variables are found in [18].

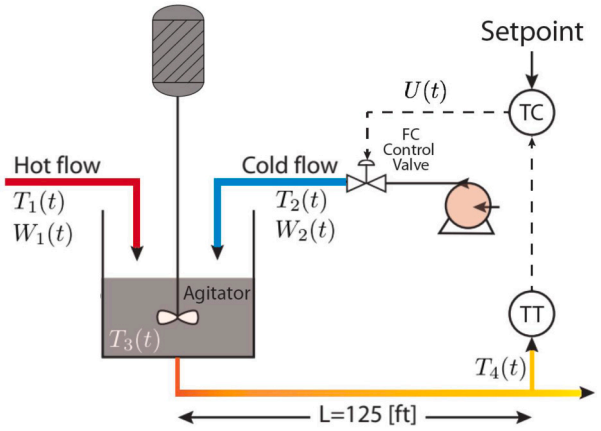

Fig. 1. Mixing tank process.

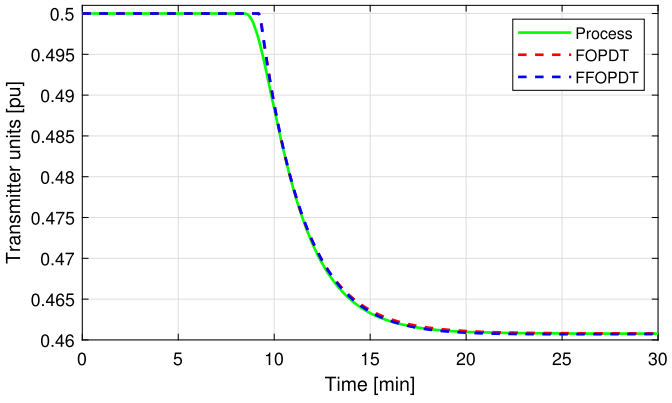

Fig. 2. Open loop response of the mixing tank process for step input.

6.1.1. *Mixing tank process identification*

Fig. 2 depicts the output of the mixed tank process and the two approximate models, FOPDT and FFOPDT. The parameters of the approximate FOPDT model were derived using the methodology proposed in [50], while those for the approximate FFOPDT model were determined using the approach presented in [23]. Equations (50) and (51) show the approximate models in the form of transfer functions.

$$G_{FOPDT}(s) = \frac{-0.8201e^{-4.2712s}}{2.1845s+1}, \tag{50}$$

$$G_{FFOPDT}(s) = \frac{-0.8201e^{-4.2391s}}{2.2649s^{1.0161}+1}. \tag{51}$$

From equations (50) and (51), the controllability index $\left(\frac{L}{T} > 1\right)$ indicates that this process is difficult to control with a dominant time delay [14]. Note also that for cases with $\frac{L}{T} > 1$, the FFOPDT model has a parameter α that is somewhat more than one.

The mean squared error (MSE) is used as an index to validate the approximate models obtained. Specifically, the results obtained for both reduced-order models, FOPDT and FFOPDT, are $MSE_{FOPDT} = 2.5127 \cdot 10^{-7}$ and $MSE_{FFOPDT} = 4.8353 \cdot 10^{-7}$, respectively. It can be seen that the value of the MSE index is very low for both approaches. Thus, the models have been validated.

6.1.2. *Fractional-order sliding mode control implementation*

In this part, the general expression for the fractional-order SMC control law is specifically expressed for the FFOPDT model considered in the application example. The approximate fractional model presented in (51) can be rewritten as a particular case:

$$G(s) = \frac{K}{(Ts^{\alpha_1}+1)(Ls^{\alpha_2}+1)} \tag{52}$$

where $K = -0.8201$, $T = 2.2649$ s, $L = 4.2391$ s, $\alpha_1 = 1.0161$, and $\alpha_2 = 1$.

The transfer function for the general fractional-order model discussed in this study is as outlined in (16). Considering the first-order approximation ($\theta = 1$) of the two-exponential function case ($n = 2$) while assuming that the truncation errors are zero, one obtains the expression:

$$U(t) = \frac{1}{K}\left[\prod_{i=1}^{2}\sum_{k=0}^{1}\frac{p_i^k}{k!}D^{k\alpha_i}X(t)\right] =$$

$$\frac{1}{K}\left[X(t) + p_1 D^{\alpha_1}X(t) + p_2 D^{\alpha_2}X(t) + p_1 p_2 D^{\alpha_1+\alpha_2}X(t)\right]. \tag{53}$$

From eq. (53), the following expression results:

$$D^{\alpha_1+\alpha_2}X(t) = \frac{K}{p_1 p_2}U(t) - \frac{1}{p_2}D^{\alpha_1}X(t) - \frac{1}{p_1}D^{\alpha_2}X(t) - \frac{1}{p_1 p_2}X(t) \tag{54}$$

Note from (52) that $p_1 = T$ and $p_2 = L$, and K, α_1 and α_2 take the numerical values above.

Next, considering $\Phi = 1$, $\Psi = 0$, and the set $A = \{\alpha_1, \alpha_2, \alpha_1 + \alpha_2\}$, the particular form of $\dot{\sigma}_\alpha\left[\mathbf{T}(e)\right](t)$ is:

$$\sum_{k\in A} a_k \frac{d}{dt}D^{\alpha_k}(R + IR - (X + IX)) =$$

$$a_0 e(t) + a_1 D^{\alpha_1}e(t) + a_2 D^{\alpha_2}e(t) + a_{12}D^{\alpha_1+\alpha_2}e(t) = 0 \tag{55}$$

Following the procedure presented in Section 4 and considering that $\alpha_1, \alpha_2 \to 1$, the derivatives approach the classical limit; therefore, we can assume that $D^{\alpha_1}R(t) = 0$, $D^{\alpha_2}R(t) = 0$, $D^{\alpha_1+\alpha_2}R(t) = 0$. In [18], it was demonstrated that the elimination of the derivatives of the reference value does not impact the performance of the control, leading to a more straightforward controller.

Remark 8. Despite the mathematical rigor employed in this work, assumptions about derivatives of the reference signal are given to simplify the practical implementation. These assumptions do not affect the development of the theory or the application itself.

From eq. (55), the following sliding condition is obtained:

$$a_0 e(t) - a_1 D^{\alpha_1}X(t) - a_2 D^{\alpha_2}X(t) - a_{12}D^{\alpha_1+\alpha_2}X(t) = 0 \tag{56}$$

Combining eqs. (53) and (56) and considering $a_{12} = 1$, we have:

$$a_0 e(t) - a_1 D^{\alpha_1}X(t) - a_2 D^{\alpha_2}X(t) -$$

$$\left[\frac{K}{p_1 p_2}U(t) - \frac{1}{p_2}D^{\alpha_1}X(t) - \frac{1}{p_1}D^{\alpha_2}X(t) - \frac{1}{p_1 p_2}X(t)\right] = 0 \tag{57}$$

Thus, the equivalent controller law is:

$$U_{eq}(t) =$$

$$\frac{p_1 p_2}{K}\left[a_0 e(t) + \left(\frac{1}{p_2} - a_1\right)D^{\alpha_1}X(t) + \left(\frac{1}{p_1} - a_2\right)D^{\alpha_2}X(t) + \frac{1}{p_1 p_2}X(t)\right] \tag{58}$$

To determine the adjusting parameters for the sliding surface, we adhere to the guidelines provided in [18]. These choices guarantee minimal performance indices and are provided as follows.

$$a_1 = \frac{1}{p_2} = \frac{1}{L} \tag{59}$$

$$a_2 = \frac{1}{p_1} = \frac{1}{T} \tag{60}$$

To ensure that the sliding surface behaves as an overdamped system, a_0 should be:

$$a_0 \leq \frac{(a_1 + a_2)^2}{4}. \tag{61}$$

Then, the resulting equivalent controller law can be rewritten as follows:

Table 1
Controller tuning parameters.

$SMC_{classic}$	$SMC_{proposed}$
$\lambda_0 = 0.1197$	$a_0 = 0.1147$
$\lambda_1 = 0.6919$	$a_1 = 0.2359$
–	$a_2 = 0.4415$
$K_D = 0.3735$	$K_D = 0.3862$
$\delta = 0.7054$	$\delta = 0.6890$

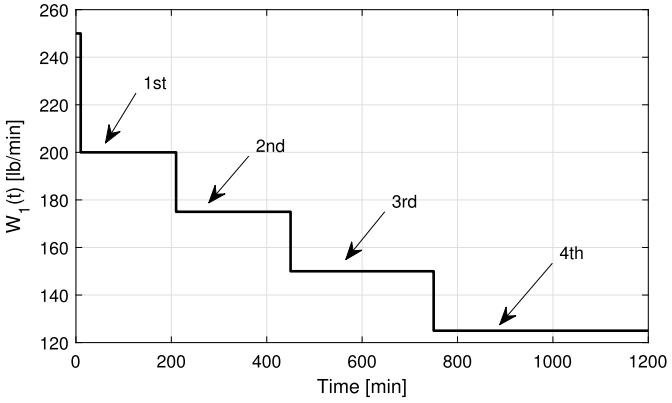

Fig. 3. Variations of hot flow $W_1(t)$.

$$U_{eq}(t) = \frac{1}{K}\left[TLa_0 e(t) + X(t)\right]. \tag{62}$$

Finally, the complete control law, the equivalent control law, and the discontinuous control law are presented in (63). Furthermore, to avoid the chattering effect, the discontinuous part is smoothed as proposed in [18]:

$$U(t) = \frac{1}{K}\left[TLa_0 e(t) + X(t)\right] + \frac{K_D \sigma_\alpha(t)}{|\sigma_\alpha(t)| + \delta}. \tag{63}$$

We compare the performance of the proposed controller with the SMC proposed in [18], called classic. Parameters K_D and δ are adjusted using the methodology described in [18]. The tuning parameters for both controllers are presented in Table 1.

6.1.3. Simulation results of mixing tank process

As mentioned above, the objective of controlling the mixing tank process is to maintain a constant required mixing temperature $T_3(t)$ in the presence of disturbances in the hot flow $W_1(t)$. Fig. 3 illustrates these disturbances in the hot flow $W_1(t)$, showing four reductions in the hot flow rate: the first, a 50 [lb/min] reduction at 10 minutes, followed by three additional reductions of 25 [lb/min] at 210, 450, and 750 minutes, respectively.

Furthermore, the adjustment made to $W_1(t)$ changes the time delay from 3 to 4.9 minutes, as illustrated in Fig. 4. Hence, the mixing tank process can be seen as a system with a variable dominant time delay.

Fig. 5 illustrates the process output in response to the disturbance rejection test, indicating that both controllers can maintain reference values in the presence of disturbances. However, the proposed controller exhibits slightly better performance during the final perturbation.

Fig. 6 shows the evolution of the control action for the disturbance rejection test, revealing that both controllers perform similarly.

Different measures, including the integral absolute error (IAE), integral square error (ISE), and the total variation of the control action (TVu), were employed to evaluate the effectiveness of both controllers. The TVu index shows comparable results for both controllers. However, the proposed controller shows slightly lower IAE and ISE values compared to the SMC controller (Fig. 7).

To assess the stability and convergence of the controller, the phase diagrams in Fig. 8 illustrate the evolution of the control law in response to each disturbance shown in Fig. 3. In this instance, the process output

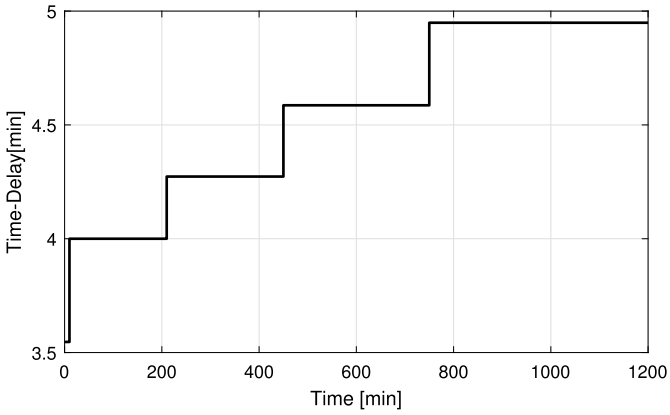

Fig. 4. Time delay variations.

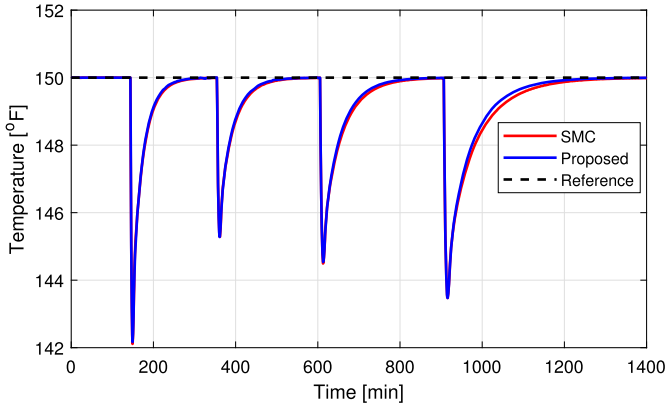

Fig. 5. Temperature responses of mixing tank process for disturbance rejection test.

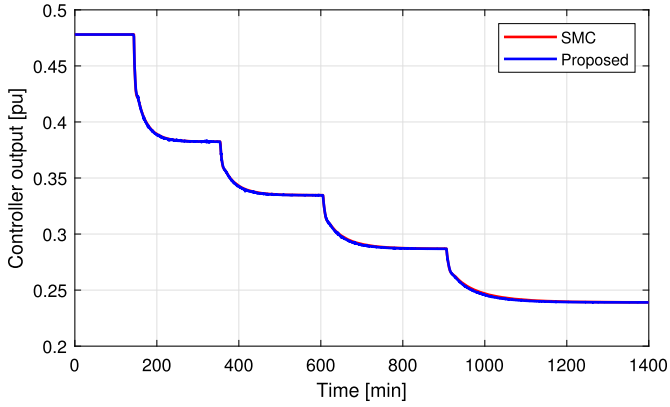

Fig. 6. Controller output for disturbance rejection test.

remains stable at the desired reference level despite the disturbances. Each disturbance causes a temporary deviation from the reference, increasing the error. However, the proposed controller ensures stable performance by showcasing a cyclic attractor that consistently converges to the same endpoint after each disturbance. The phase diagrams effectively demonstrate the controller's capability to restore the process to the reference level following disturbances and variations in the nominal dead time.

6.2. High-order linear system with a long time delay

This numerical example was previously studied by Camacho et al. in [51] and its transfer function is presented below:

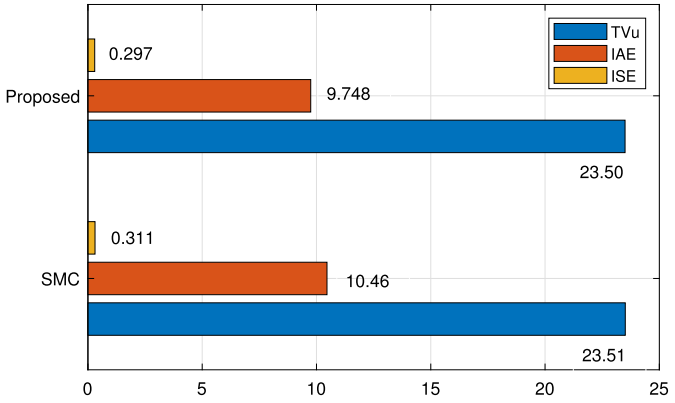

Fig. 7. Comparative of performance indexes of the controllers for disturbance rejection test.

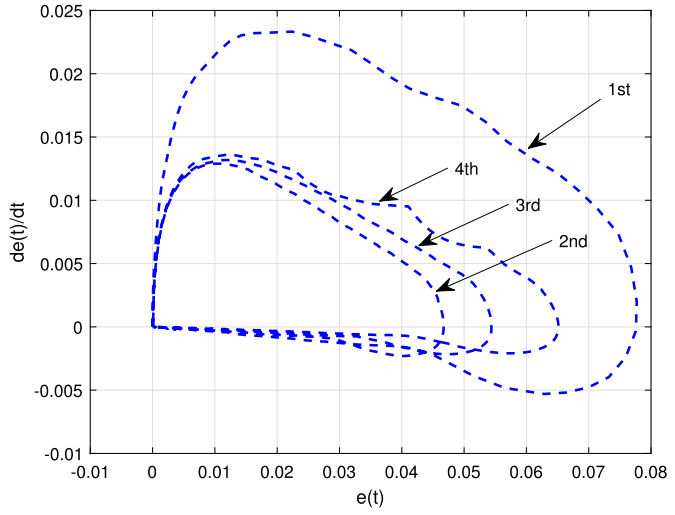

Fig. 8. A phase-portraits for each disturbance of Fig. 3.

$$G(s) = \frac{e^{-5s}}{(s+1)(0.5s+1)(0.25s+1)(0.125s+1)} \tag{64}$$

The system represented in Eq. (64) can be approximated by an FOPDT model using the reaction curve method [49], as follows:

$$G_{FOPDT}(s) = \frac{e^{-5.68s}}{1.3s+1} \tag{65}$$

For the fractional model, the method proposed by Gude in [23] is used to obtain the parameters of the FFOPDT model:

$$G_{FFOPDT}(s) = \frac{e^{-5.469s}}{1.668s^{1.124}+1} \tag{66}$$

As evident from the above equations, the controllability ratio $\frac{L}{T} > 1$ suggest that the process is difficult to control. Additionally, for these cases, the FFOPDT model exhibits a parameter α slightly greater than 1.

Fig. 9 shows the open-loop process output response, alongside the responses of the FOPDT and FFOPDT models for a step input. To validate the approximate models, the mean square error (MSE) was calculated, resulting in $MSE_{FOPDT} = 1.721 \cdot 10^{-4}$ and $MSE_{FFOPDT} = 4.718 \cdot 10^{-4}$. Both models exhibit low MSE values, indicating that they are well-validated.

6.2.1. Implementation of the proposed control

To implement the proposed controller for high-order linear systems with a long time delay, the procedure outlined in Section 6.1.2 is followed. Using the approximate fractional model from (66), the following parameters are obtained: $K = 1$, $T = 1.668$ s, $L = 5.469$ s, $\alpha_1 = 1.124$, and $\alpha_2 = 1$. Additionally, the first-order approximation ($\theta = 1$) of the two-exponential function case ($n = 2$) is analyzed under the assumption of zero truncation errors. In this particular case, $\Phi = 1$ and $\Psi = 0$ are considered with the set $A = \{\alpha_1, \alpha_2, \alpha_1 + \alpha_2\}$.

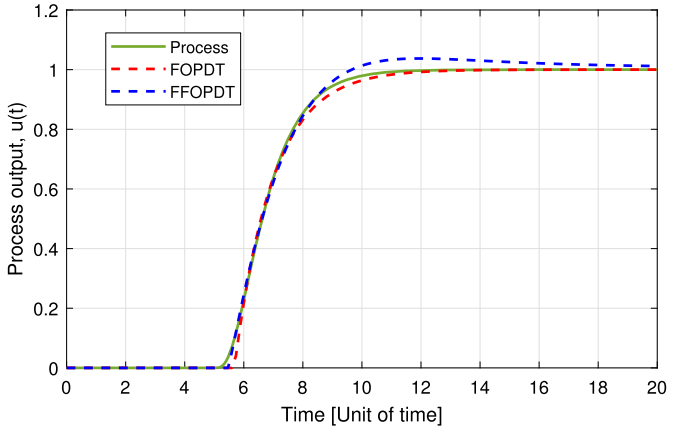

Fig. 9. Open-loop output response of high-order linear system with a long time delay for step input.

Table 2
Controller parameters for high-order linear system with a long time delay.

$SMC_{classic}$	$SMC_{proposed}$
$\lambda_0 = 0.2011$	$a_0 = 0.1377$
$\lambda_1 = 0.9453$	$a_1 = 0.1828$
–	$a_2 = 0.5994$
$K_D = 0.1663$	$K_D = 0.2069$
$\delta = 0.6989$	$\delta = 0.6845$

To adjust the sliding surface parameters, we follow the guidelines provided in [18]. To achieve optimal performance indices and ensure that the system exhibits overdamped behavior, the relationships specified in (59), (60), and (61) are applied.

The sliding surface is then defined similarly to (55), and the corresponding control law is given in (63).

We compare the performance of the proposed controller with the conventional SMC outlined in [18]. The parameters K_D and δ are optimized using the approach described in [18]. The tuning parameters for both controllers are presented in Table 2.

6.2.2. Reference tracking test

In this test, two reference changes are introduced. The first is a unit step applied at 5 [sec], while the second involves reducing the amplitude to 0.5 at 160 [sec], which is maintained until the end of the simulation, as shown in Fig. 10. Both controllers successfully guide the process to track the reference. Additionally, the proposed controller shows a lower overshoot compared to the SMC during the reference changes.

Fig. 11 presents the responses of the control actions. It is observed that the SMC controller generates larger control action peaks compared to the proposed controller during the reference changes.

The performance metrics for the reference tracking test are shown in Fig. 12, where it can be seen that the proposed controller has the lowest values in terms of the performance indices TVu, ISE, IAE and overshoot $M_p\%$. This indicates that the proposed controller provides better overall performance.

6.2.3. Disturbance rejection test

In this test, a unit step reference change is applied at 5 [sec], followed by a disturbance with an amplitude of −0.2, introduced at 160 [sec] and maintained until the end of the simulation, as shown in Fig. 13. Both

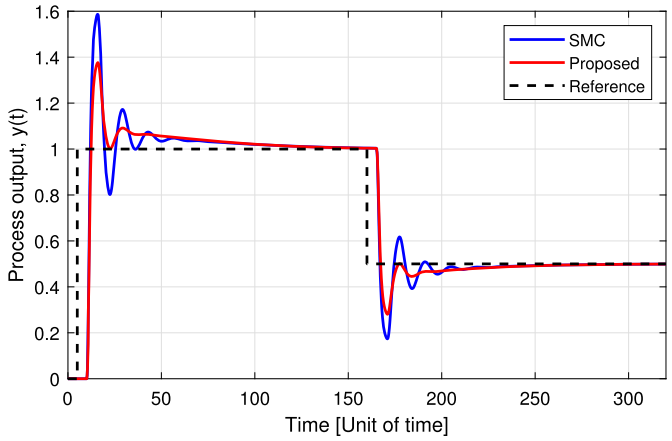

Fig. 10. Output responses for reference tracking test.

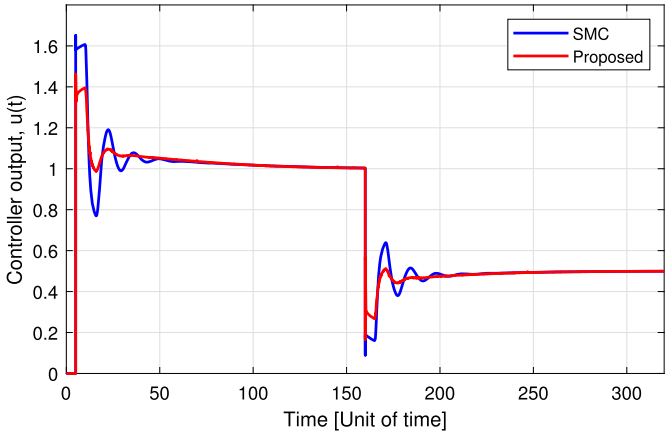

Fig. 11. Control action responses for reference tracking test.

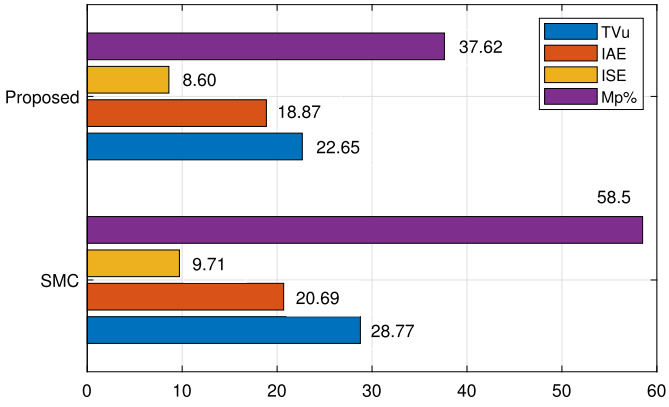

Fig. 12. Comparative of performance indexes of the controllers for reference tracking test.

controllers successfully reject the disturbance while maintaining the desired reference, with similar output responses during the disturbance.

Fig. 14 shows the control action for the disturbance test, showing that both controllers produce very close responses when the disturbance occurs.

Fig. 15 provides a detailed comparison of the performance indices obtained for the disturbance test. It is evident that both controllers perform similarly, with very similar values in terms of IAE, ISE, and TVu.

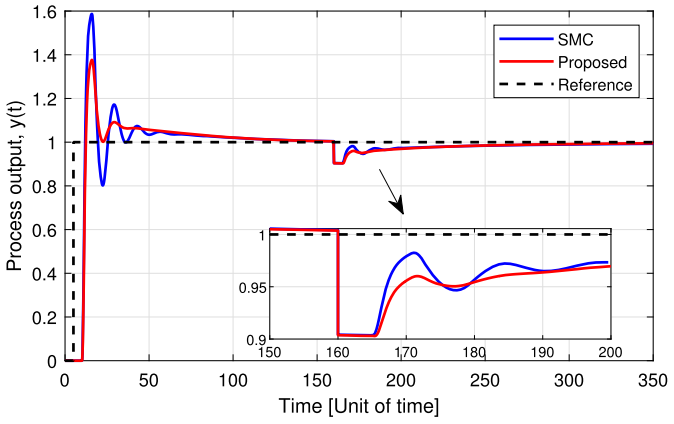

Fig. 13. Output Responses for disturbance test.

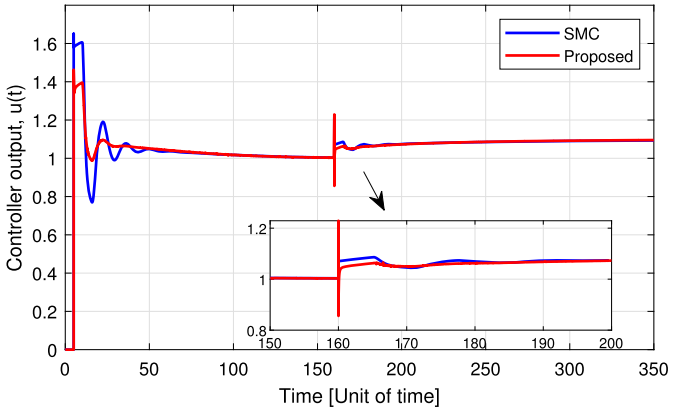

Fig. 14. Control action responses for disturbance test.

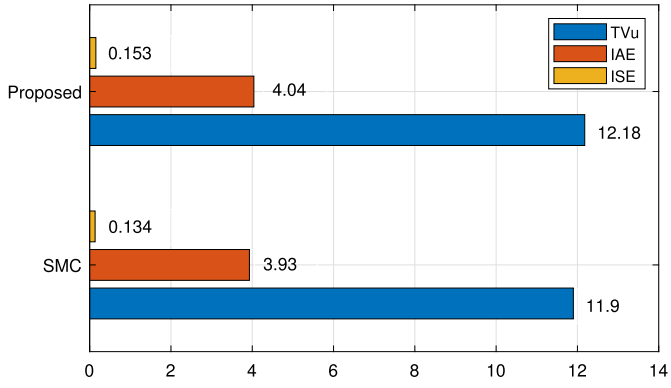

Fig. 15. Comparative of performance indexes of the controllers for disturbance test.

To summarize, the proposed controller outperforms the original one in the tracking test and yields comparable results in the disturbance rejection test. Thus, the generalized model's proposed controller is effective for processes with variable and dominant delays.

7. Conclusions

This article presented preliminary findings from a study evaluating the potential advantages of adopting a unified, systematic, and organized general reduced-order fractional model within the SMC design framework.

The simulation findings showed that, compared to an SMC based on an FOPDT model, the proposed SMC, considering the generalized

fractional model, performed slightly better in handling disturbances with different dead-time variations. The proposed controller also outperformed the conventional SMC for high-order systems with long delay, particularly in reference tracking. Future studies should explore a wider variety of evaluations, including the effects of noise, the time required to attain the sliding surface, and controller tuning equations derived from fractional parameters obtained through the identification methodology.

CRediT authorship contribution statement

Juan J. Gude: Writing – review & editing, Writing – original draft, Validation, Software, Methodology, Investigation, Conceptualization. **Antonio Di Teodoro:** Writing – review & editing, Writing – original draft, Methodology, Investigation, Conceptualization. **D'hamar Agudelo:** Writing – review & editing, Writing – original draft, Visualization, Software, Investigation. **Marco Herrera:** Writing – review & editing, Methodology, Investigation, Data curation. **Luis Rincón:** Writing – review & editing, Software, Investigation. **Oscar Camacho:** Writing – review & editing, Writing – original draft, Project administration, Methodology, Investigation, Formal analysis, Conceptualization.

Declaration of competing interest

The authors declare that they have no known competing financial interests or personal relationships that could have appeared to influence the work reported in this paper.

Data availability

No data was used for the research described in the article.

Acknowledgement

The Colegio de Ciencias e Ingenieras of the Universidad San Francisco de Quito USFQ provided support for this research through the Poli-Grants Program, Grant No. 24280.

Juan J. Gude acknowledges funding support from the Basque Government through the BEREZ-IA Elkartek project (ref. KK-2023/00012).

Marco Herrera thanks the Advanced Control Systems Research Group at USFQ for providing a research internship.

References

[1] B.J. West, Fractional Calculus and the Future of Science, MDPI, Basel, 2022.
[2] K. Diethelm, V. Kiryakova, Y. Luchko, J.T. Machado, V.E. Tarasov, Trends, directions for further research, and some open problems of fractional calculus, Nonlinear Dyn. 107 (4) (2022) 3245–3270.
[3] C.A. Monje, Y. Chen, B.M. Vinagre, D. Xue, V. Feliu-Batlle, Fractional-Order Systems and Controls: Fundamentals and Applications, Springer Science & Business Media, 2010.
[4] H. Sun, Y. Zhang, D. Baleanu, W. Chen, Y. Chen, A new collection of real world applications of fractional calculus in science and engineering, Commun. Nonlinear Sci. Numer. Simul. 64 (2018) 213–231.
[5] K.M. Saad, A different approach for the fractional chemical model, Rev. Mex. Fis. 68 (1) (0–0 2022).
[6] A.L. Ferrari, M.C.S. Gomes, A.C.R. Aranha, S.M. Paschoal, G. de Souza Matias, L.M. de Matos Jorge, R.O. Defendi, Mathematical modeling by fractional calculus applied to separation processes, Sep. Purif. Technol. (2024) 126310.
[7] G. de Souza Matias, C.A. Bissaro, L.M. de Matos Jorge, D.F. Rossoni, The fractional calculus in studies on drying: a new kinetic semi-empirical model for drying, J. Food Process Eng. 42 (1) (2019) e12955.
[8] P. Shah, R. Sekhar, D. Sharma, H.R. Penubadi, Fractional order control: a bibliometric analysis (2000–2022), in: Results in Control and Optimization, 2023, 100366.
[9] F. Padula, A. Visioli, et al., Advances in Robust Fractional Control, Springer, 2015.
[10] Y. Chen, I. Petras, D. Xue, Fractional order control-a tutorial, in: 2009 American Control Conference, IEEE, 2009, pp. 1397–1411.
[11] B. Shi, J. Yuan, C. Dong, et al., On fractional model reference adaptive control, Sci. World J. (2014) 2014.
[12] A. Tepljakov, B.B. Alagoz, C. Yeroglu, E.A. Gonzalez, S.H. Hosseinnia, E. Petlenkov, A. Ates, M. Cech, Towards industrialization of fopid controllers: a survey on milestones of fractional-order control and pathways for future developments, IEEE Access 9 (2021) 21016–21042.
[13] A. Di Teodoro, M. Herrera, L. Rincon, J.J. Gude, O. Camacho, A hybrid control framework for chemical processes with long time delay: theory and experiments, ACS Omega 9 (30) (2024) 32469–32480.
[14] K.J. Åström, T. Hägglund, Advanced PID Control, ISA-the Instrumentation, Systems and Automation Society, 2006.
[15] A. Tepljakov, B.B. Alagoz, C. Yeroglu, E. Gonzalez, S.H. HosseinNia, E. Petlenkov, Fopid controllers and their industrial applications: a survey of recent results, IFAC-PapersOnLine 51 (4) (2018) 25–30.
[16] J.J. Gude, E. Kahoraho, Simple tuning rules for fractional pi controllers, in: 2009 IEEE Conference on Emerging Technologies & Factory Automation, IEEE, 2009, pp. 1–8.
[17] J.J. Gude, E. Kahoraho, Modified Ziegler-Nichols method for fractional pi controllers, in: 2010 IEEE 15th Conference on Emerging Technologies & Factory Automation (ETFA 2010), IEEE, 2010, pp. 1–5.
[18] O. Camacho, C.A. Smith, Sliding mode control: an approach to regulate nonlinear chemical processes, ISA Trans. 39 (2) (2000) 205–218.
[19] M.F. Sardella, M.E. Serrano, O. Camacho, G.J. Scaglia, Design and application of a linear algebra based controller from a reduced-order model for regulation and tracking of chemical processes under uncertainties, Ind. Eng. Chem. Res. 58 (33) (2019) 15222–15231.
[20] A. Tepljakov, Fractional-Order Modeling and Control of Dynamic Systems, Springer, 2017.
[21] I. Petráš (Ed.), Handook of Fractional Calculus with Applications. Applications in Control, Volume 6, De Gruyter, Berlin, Boston, 2019, https://doi.org/10.1515/9783110571745.
[22] J.J. Gude, Contributions to Fractional-Order Modelling and Control of Dynamic Systems: A Theoretical and Practical Approach, University of Deusto, 2023.
[23] J.J. Gude, P. García Bringas, Influence of the selection of reaction curve's representative points on the accuracy of the identified fractional-order model, J. Math. 2022 (2022).
[24] J.J. Gude, P. García Bringas, Proposal of a general identification method for fractional-order processes based on the process reaction curve, Fractal Fract. 6 (9) (2022) 526.
[25] J.J. Gude, A. Di Teodoro, O. Camacho, P. García Bringas, A new fractional reduced-order model-inspired system identification method for dynamical systems, IEEE Access (2023).
[26] E. Guevara, H. Meneses, O. Arrieta, R. Vilanova, A. Visioli, F. Padula, Fractional order model identification: computational optimization, in: 2015 IEEE 20th Conference on Emerging Technologies & Factory Automation (ETFA), IEEE, 2015, pp. 1–4.
[27] B.B. Alagoz, A. Tepljakov, A. Ates, E. Petlenkov, C. Yeroglu, Time-domain identification of one noninteger order plus time delay models from step response measurements, Int. J. Model. Simul. Sci. Comput. 10 (01) (2019) 1941011.
[28] J.J. Gude, P. García Bringas, M. Herrera, L. Rincón, A. Di Teodoro, O. Camacho, Fractional-order model identification based on the process reaction curve: a unified framework for chemical processes, Results Eng. (2024) 101757.
[29] J.J. Gude, P. García Bringas, A novel control hardware architecture for implementation of fractional-order identification and control algorithms applied to a temperature prototype, Mathematics 11 (1) (2022) 143.
[30] M.W.S. Campos, F.A.C. Ayres Jr, I.V. de Bessa, R.L.P. de Medeiros, P.R.O. Martins, E. kaminski Lenzi, J.E.C. Filho, J.R.S. Vilchez, V.F. Lucena Jr, Fractional-order identification system based on Sundaresan's technique, Chaos Solitons Fractals 185 (2024) 115132.
[31] C.I. Muresan, I. Birs, C. Ionescu, E.H. Dulf, R. De Keyser, A review of recent developments in autotuning methods for fractional-order controllers, Fractal Fract. 6 (1) (2022) 37.
[32] A.M. Nassef, M.A. Abdelkareem, H.M. Maghrabie, A. Baroutaji, Metaheuristic-based algorithms for optimizing fractional-order controllers—a recent, systematic, and comprehensive review, Fractal Fract. 7 (7) (2023) 553.
[33] O. Naifar, A.B. Makhlouf, Fractional Order Systems–Control Theory and Applications, Springer, 2022.
[34] D. Xue, Fractional-Order Control Systems: Fundamentals and Numerical Implementations, vol. 1, Walter de Gruyter GmbH & Co KG, 2017.
[35] V. Utkin, A. Poznyak, Y.V. Orlov, A. Polyakov, Road Map for Sliding Mode Control Design, Springer, 2020.
[36] J.-J.E. Slotine, W. Li, et al., Applied Nonlinear Control, vol. 2, Prentice Hall, Englewood Cliffs, NJ, 1991.
[37] A. Mehta, B. Bandyopadhyay, Emerging trends in sliding mode control, Stud. Syst. Decis. Control 318 (2021).
[38] J. Liu, X. Wang, J. Liu, X. Wang, Advanced Sliding Mode Control, Springer, 2011.
[39] C. Kadu, A. Khandekar, C. Patil, Design of sliding mode controller with proportional integral sliding surface for robust regulation and tracking of process control systems, J. Dyn. Syst. Meas. Control 140 (9) (2018) 091004.
[40] J. Espín, S. Estrada, D. Benítez, O. Camacho, A hybrid sliding mode controller approach for level control in the nuclear power plant steam generators, Alex. Eng. J. 64 (2023) 627–644.
[41] D. Cargua-Sagbay, E. Palomo-Lema, O. Camacho, H. Alvarez, Flash distillation control using a feasible operating region: a sliding mode control approach, Ind. Eng. Chem. Res. 59 (5) (2020) 2013–2024.
[42] O.E. Camacho, C. Smith, E. Chacón, Toward an implementation of sliding mode control to chemical processes, in: ISIE'97 Proceedings of the IEEE International Symposium on Industrial Electronics, IEEE, 1997, pp. 1101–1105.

[43] M. Vásquez, J. Yanascual, M. Herrera, A. Prado, O. Camacho, A hybrid sliding mode control based on a nonlinear PID surface for nonlinear chemical processes, Int. J. Eng. Sci. Technol. 40 (2023) 101361.
[44] S. Li, P. Li, Z. Zheng, T. Huang, Fractional order sliding mode control for circulating current suppressing of mmc, Electr. Eng. 105 (6) (2023) 3791–3800.
[45] A.A. Kilbas, H.M. Srivastava, J.J. Trujillo, Theory and Applications of Fractional Differential Equations, vol. 204, Elsevier, 2006.
[46] K.S. Miller, B. Ross, An Introduction to the Fractional Calculus and Fractional Differential Equations, Wiley, 1993.
[47] I. Podlubny, Fractional-order systems and fractional-order controllers, Institute of Experimental Physics, Slovak Academy of Sciences, Kosice 12 (3) (1994) 1–18.
[48] A.A. Kilbas, O. Marichev, S. Samko, in: Fractional Integrals and Derivatives (Theory and Applications), 1993.
[49] B.G. Liptak, M.J. Piovoso, F.G. Shinskey, H. Eren, G.K. Totherow, J.E. Jamison, D. Morgan, H.I. Hertanu, E.M. Marszal, J. Berge, et al., Instrument Engineers' Handbook, Volume Two: Process Control and Optimization, CRC Press, 2018.
[50] V.M. Alfaro, Identificación de modelos de orden reducido a partir de la curvatura de reacción del proceso, Cienc. Tecnol. 24 (2) (2006).
[51] O. Camacho, R. Rojas, W. García-Gabín, Some long time delay sliding mode control approaches, ISA Trans. 46 (1) (2007) 95–101.